Powder Technology, 9 (1974) 199—211

Characterization of the Compaction and Sintering of Hydroxyapatite Powders by Mercury Porosimetry*

HILLAR M. ROOTARE** and ROBERT G. CRAIG

Department of Dental Materials, University of Michigan, School of Dentistry, Ann Arbor, Mich. 48104 (U.S.A.)

(Received May 25, 1973; in revised form November 26, 1973)

Summary

Mercury porosimetry was used to measure the bulk and real densities, pore volumes and pore size distributions of compacts of hydroxyapatite before and after sintering. The hydroxyapatites were prepared by two different methods and had widely different surface areas. The properties were determined as a function of compaction force and sintering temperature. Densities from porosimetry were in good agreement with geometric densities. A linear relation was found between pore volume and log of the applied force. There was also a linear relationship between bulk volume and pore volume of the compacts. A bimodal pore size distribution was observed for the high surface area hydroxyapatite which disappeared with increasing compaction loads. Pressurization and depressurization measurements indicated that the main body of the pores in the compacts attained a more regular "spherical" shape with increasing compaction force than did the "necks". The pore volume, percent porosity, and bulk density of the compacts remained unchanged up to 600°C; however, the surface area and the average pore diameter changed at 400°C. The distribution of pores became more uniform, narrower in distribution, and larger in size as the sintering temperature increased. The change in pore area with pore volume indicated that two mechanisms were operating during sintering. The pore area proved to be the most sensitive indicator of changes during sintering.

1. INTRODUCTION

Hydroxyapatite (HAP) is the principal inorganic component of teeth and bone. Dentin, cementum and enamel are the three types of hard tissue composing teeth. A soft, nonmineralized tissue, dental pulp, is enclosed centrally within the hard tissue. Dentin is composed of about 69% mineral, 18% organic phase, and 13% of water by weight. Cementum covers the root portion of the dentin while enamel covers the crown portion. Cementum is softer than dentin and is composed of 46% mineral, 22% organic phase and 32% water. Enamel consists of approximately 96% mineral, 1.7% organic phase and 2.3% water [1].

This study is concerned with the mineral portion of the tooth structure common to all three dental hard tissues which is apatitic in nature. Its composition is that of mostly calcium hydroxyapatite with inclusions of impurities such as magnesium, strontium, sodium, carbonate, fluorine and chlorine. Tin, lead, copper, zinc and iron have also been found in small quantities. Hydroxyapatite (HAP) refers to crystalline material with the unit cell formula of $Ca_{10}(PO_4)_6(OH)_2$ [2,3]. A much larger class of materials is covered by the term apatite*, and frequently the general-

* Taken from a dissertation submitted in partial fulfilment of the Ph.D. degree in dental materials and pharmaceutical chemistry at the University of Michigan, 1973.

** Present address: The L.D. Caulk Co., P.O. Box 359, Milford, Del. 19963, U.S.A.

* Apatite is from the Greek word *apate*, which means deceit. The name was given because apatite was often mistaken for other minerals. Fluorapatite in particular comes in many colors: white, yellow, blue, green, brown, etc.

TABLE 1
Physical properties of hydroxyapatite powders

HAP	Pore volume		Bulk density	Density	Surface area	Median pore diam.	Mean particle size	
	(cm^3/g)	(%)	(g/cm^3)	(g/cm^3)	(m^2/g)	(μm)	$\bar{X}_g(\mu m)$	$\pm\sigma_g$
VIC	1.337	78.3	0.586	2.70	70.4	0.27	8.5	2.4
TVA	0.776	70.7	0.911	3.11	3.0	5.1	16.0	1.3

ized term may be used to describe any calcium orthophosphate precipitate that yields an X-ray diffraction pattern similar to that of HAP. Apatites deviate from the ideal composition, or the molar calcium - phosphate ratio (Ca/P) of 1.667, either in calcium or phosphate content by inclusion of contaminants and other ions such as F^-, Cl^-, CO_3^{2-}, Mg^{2+}, Na^+ or H_2O that is tightly held within the crystal.

There is a need for a strong, inert, biologically compatible material for implants to replace teeth or bone lost as a result of disease or accident [4 - 6]. All human hard tissues are composed of HAP as one of the main mineral phases. The understanding of the technique of fabricating synthetic HAP powders into hard, porous appliances is a logical initial step in exploring the feasibility of the materials as implants. Information about the particle size of the powder and pore size distributions within the compacts before and after sintering is important in the development of HAP ceramic implants.

2. MATERIALS AND METHODS

2.1 Hydroxyapatite powders

Two hydroxyapatite samples were used in the compaction study, VIC-HAP* and TVA-HAP**. VIC-HAP was a commercial product prepared by precipitation from hot water, which resulted in a finely powdered sample with 50% of the particles with dimensions less than 8.5 μm. The sample had a low bulk density and a high surface area.

The TVA-HAP sample was prepared by a high temperature solid state reaction according to the method developed at the Tennessee Valley Authority (TVA) Fundamental Research Branch. It consisted of heating a stoichiometric mixture of monocalcium phosphate monohydrate $Ca(H_2PO_4)_2.H_2O$ and calcium carbonate at 1200°C in an atmosphere of equal volumes of steam and nitrogen for three hours. The TVA-HAP sample had a low surface area of 3.0 m^2/g and a Ca/P ratio of 1.665. Table 1 lists some of the physical properties of the HAP samples.

2.2 Compaction of hydroxyapatite powders

Since the most abundant sample was VIC-HAP, most of the data on compaction and sintering of the compacts were obtained on that sample. There was only a small supply of TVA-HAP available. Enough data, however, were collected on TVA-HAP in order to establish a relationship between the compactibility of the two different hydroxyapatite samples.

The powders were compacted in a 1/2-in.-diam. steel die using a 5000-lb. capacity Riehle Tensile and Compression Testing Machine* as a press. The 5000-lb. pressure range was divided into five scales, each of which could be read with a precision of 0.1%. Because of the fixed die size, the measurement of the diameter did not change significantly from pellet to pellet. The only dimension that varied was the height of the pellet, and this changed with the amount of the powder used and the force applied during compaction.

The effect of the compaction force on the process of forming the pellet was to be evaluated, and therefore an attempt was made to keep the mass of the sample constant, about 0.35 g. The effect of the variation of the mass was not investigated. The powdered samples were weighed with a Mettler M5 Microbal-

* Victor Division, Stauffer Chemical Co., 380 Madison Ave., New York, N.Y. 10017.

** Tennessee Valley Authority, Report No. 678, November 6, 1956, Wilson Dam, Alabama.

* Ametek, Inc., Riehle Testing Machines, 554 12th Ave., E. Moline, Illinois.

TABLE 2
Bulk density of VIC- and TVA-HAP compacts

Compact	Geometrical G(g/cm³)	Mercury M(g/cm³) VIC	G/M	Geometrical G(g/cm³)	Mercury M(g/cm³) TVA	G/M
100P	0.842	0.825	1.021			
250P	0.936	0.925	1.012			
500P	1.042	1.023	1.019	1.322	1.312	1.008
1000P	1.170	1.139	1.027	1.471	1.459	1.008
2000P	1.311	1.295	1.027	1.618	1.593	1.016
3000P	1.414	1.365	1.036	1.734	1.705	1.017
5000P	1.542	1.497	1.030	1.856	1.816	1.022
			$\bar{X}$ = 1.022 ± .003			$\bar{X}$ = 1.014 ± .003
			C.V. = 0.33%			C.V. = 0.27%

ance* which had a total capacity of 20 g and a precision of ± 0.001 mg. As a result of the limited precision of the micrometer used to measure the thickness of the compacts, the values for the sample weights were rounded off to the nearest fourth decimal place.

The powders were compressed in the die at loads indicated in Table 2 with the suffix P after the numerical value of the load in pounds, for example 100P, 500P and 1000P. The powder was kept at the fixed load and the press was adjusted to keep it constant, until no flow was indicated. The time to reach no observable flow varied from one-half to one minute, and an extra minute under the load was allowed for compaction. The total time under compression at each load was approximately 2 minutes.

The die was carefully made to keep the piston and the anvil surfaces parallel; nevertheless, the thickness measurements on the compacts were made at five places and these values averaged. The center of the pellet and the edges at four cardinal headings (90° apart) were measured for thickness with a micrometer. Usually no significant differences in thickness were found, but some difference occasionally occurred as a result of the unevenly distributed powder bed in the bottom of the die.

2.3 Mercury porosimetry

The mercury intrusion method is commonly used to characterize pore size distribution in a porous sample by means of a mercury porosimeter [7 - 10]. A porosimeter is a device capable of generating suitably high pressures, and the volume of mercury forced into the pores of the sample is measured. The volume change with an increase in pressure was measured by a capacitance bridge. The capacitance change between the column of mercury in the dilatometer stem and an external shield around the penetrometer was measured and related directly to the volume change. The 60,000 psi mercury porosimeter* used in this study utilized such a capacitance bridge. This instrument will measure pore size distributions from 100 μm to 30 Å in diameter, Other instruments are also available**.

The instrument incorporates two independent pressure systems. One is for the evacuation of the sample, filling the penetrometer with mercury and pressurizing the sample to atmospheric pressure, by allowing air to flow through the stopcock of the filling device. This system fills the pores from 100 μm to 18 μm in diameter. The other pressure system is for pressurizing the sample from atmospheric pressure to 60,000 psi, which extends the range of pore sizes intruded by mercury from 18 μm to 30 Å in diameter.

The pressure in the filling device is mea-

* Mettler Instrument Corp., 20 Nassau Street, Princeton, New Jersey 08540.

* Aminco, Model 5—7125B. American Instrument Co., 8030 Georgia Ave., Silver Spring, Md. 20910.

** Other manufacturers of mercury porosimeters are Carlo Erba Scientific Instruments Division, Via Carlo Imbonati, 24 I 20159 Milano, Italy (porosimeter model 70 has max. pressure 3000 kg/cm² and pore range 37.5 Å to 75 μm) and Micromeritics Instrument Corp., 800 Goshen Springs Road, Norcross, Ga. 30071 (porosimeter model 905 has max. pressure 50,000 psi and pore range 35 Å to 177 μm).

sured by a thermocouple vacuum gauge (0 - 1000 μm) during the outgassing of the sample in the filling device, and a sub-atmospheric (0 - 15 psi) pressure gauge that reads in 0.05-psi increments with an accuracy of ¼% of full scale reading. In the high pressure vessel, the system pressure is monitored by an intermediate 0 - 5000 psi gauge, that enables measurements of low pressures to the nearest 2.5 psi up to 5000 psi with an accuracy of 0.1% of the full scale reading. Higher pressures are read from 0 to 60,000 psi gauge to the nearest 50 psi with an accuracy of 0.1% of the full scale reading.

The volume change in the penetrometer is measured visually in the filling device, and by the capacitance bridge in the pressure vessel. The calibrated stem volume of a standard penetrometer is 0.200 cm^3, and is visually readable in 0.001-cm^3 increments. With the capacitance sheath, the total measurable intrusion volume of the stem is 0.3000 cm^3 and is readable in 0.0001-cm^3 increments.

3. EXPERIMENTAL

3.1 Bulk density and bulk volume measurements of VIC- and TVA-HAP compacts

The bulk geometric volume and density were calculated using five replications of sample compacts at each pressure, when sample supply was available. Bulk geometric densities of VIC- and TVA-HAP compacts are listed in Table 2. The bulk geometric volume is simply the reciprocal of the bulk geometric density. The reproducibility of the geometric bulk density determination was very good, varying between 0.1 and 0.2%.

Since the remainder of the characterization of the compacts was to be conducted by mercury porosimetry, it was important to determine how well the geometric bulk density measurements correlated with the values determined from porosimetry. The bulk density data determined by the two methods for both VIC- and TVA-HAP are listed in Table 2.

The ratio of the geometric to mercury porosimetry (G/M) bulk densities was approximately 1.02. The coefficient of variation (C.V.) for the data was 0.3%. It is also noteworthy that the C.V. for VIC- and TVA-HAP was about the same. The bulk densities by the two methods were nearly identical for both

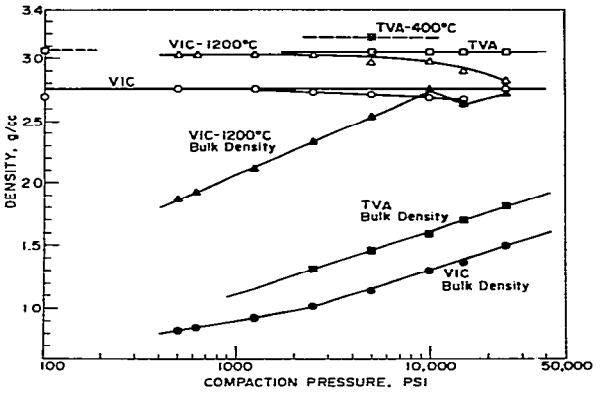

Fig. 1. Bulk and real densities of hydroxyapatites before and after sintering as a function of log of compaction pressure.

samples. These data established not only the reproducibility of the two methods for measuring the bulk density of the compacts, but also substantiated the reliability of using mercury porosimetry data in measuring bulk densities.

Semi-log plots of the bulk and real densities of the compacts, measured by mercury porosimetry, as a function of compaction pressure are shown in Fig. 1. Data for VIC-HAP are plotted on a magnified scale in Fig. 2, which show the variation of the bulk and real density with the compaction force. It is noteworthy that while the bulk density of the compacts steadily increased with load, the porosimetry density decreased sharply before returning to its true value of about

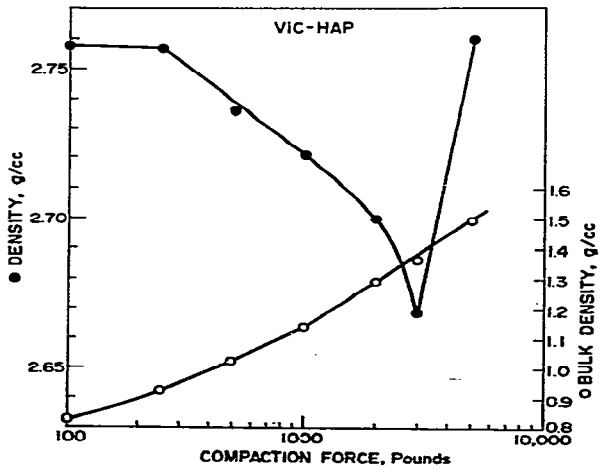

Fig. 2. Porosimetry density and bulk density of VIC-HAP as a function of compaction force.

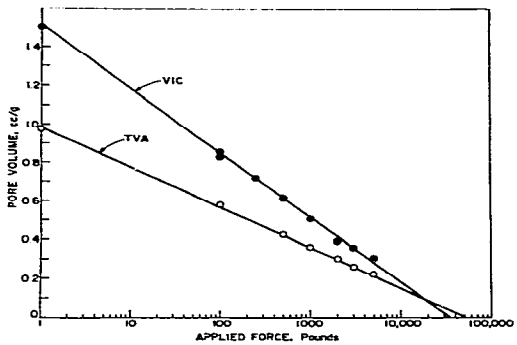

Fig. 3. Pore volumes of VIC- and TVA-HAP powder and compacts as a function of log of applied force (lb.) on the ½-in. die in compaction.

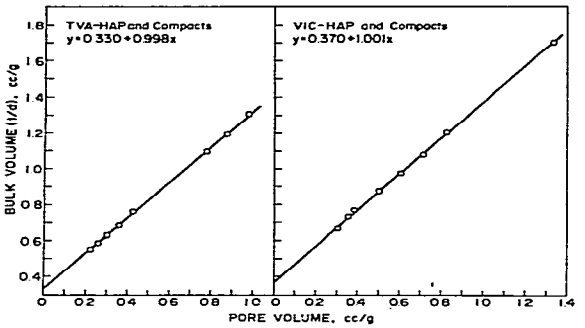

Fig. 4. Linear relationship between bulk volume ($1/d$) and pore volume for the powder and compacts of TVA- and VIC-HAP samples.

2.76 g/cm^3. It can be deduced from these data that the measurement of real density is much more sensitive to the closing of the void spaces between particles, and forming closed pores, than measurement of the bulk density.

3.2 Pore volume of VIC- and TVA-HAP compacts

Another important parameter in compaction of powders that must be measured and controlled is the pore volume of the compact. Semi-log plots of pore volumes *versus* compaction force for both VIC- and TVA-HAP compacts are presented in Fig. 3. A linear relationship between pore volume of the compact and the log of the applied force during compaction was established for both VIC- and TVA-HAP samples. The two slopes were different because of differences in the powder characteristics and the particle size distributions.

The linear relationship allows the selection of conditions for compaction in order to obtain a compact of desired pore volume or porosity. Also, by extrapolation it was determined that approximately 35,000 and 55,000 lb. of force applied on a ½-in. die was required to form a completely densified compact of VIC- and TVA-HAP, respectively. In terms of pressure these forces are equivalent to 175,000 and 275,000 psi.

Any desired pore volume (P.V.) for the compact can be calculated from the linear relationships:

VIC-HAP P.V. = (1.498 ± 0.032) — (0.1426 ± 0.0047) ln Force

TVA-HAP P.V. = (0.9430 ± 0.0313) — (0.0844 ± 0.0042) ln Force

Linear pore volume relationships could be established for other powder samples in a similar manner.

Another interesting observation resulting from study of the compaction of hydroxyapatite powders was the linear relationship between bulk volume and pore volume, and these data are plotted in Fig. 4. There is a one-to-one correspondence between change in bulk volume and change in pore volume, regardless of the sample powder. Slopes for both VIC- and TVA-HAP are about 1.00; however, intercepts of these lines on the ordinate (bulk volume) differ. This type of plot is not sensitive to differences in particle size distribution, but only to the true density of the solid. Since bulk volume is the reciprocal of bulk density, it will yield the true density of the solid from the intercept of this line, when the pore volume becomes zero. Similar plots, therefore, can be made for any powder in compaction by knowing the true density, and using a straight line of a slope of one. This type of plot can be useful in connection with the plot in Fig. 3 to design conditions for compaction of a powder, in order to obtain a compact of specific bulk density or pore volume.

By linear regression of these data, the measured bulk densities yield a good estimate of the true density of each hydroxyapatite powder. For VIC-HAP the true density was calculated to be 2.70 ± 0.05 g/cm^3, and for the TVA-HAP it was 3.03 ± 0.04 g/cm^3. These values agree quite well with the independently determined density values for each individual compact, which ranged from 2.67 to 2.76 g/cm^3 for VIC-HAP, and from 2.95 to

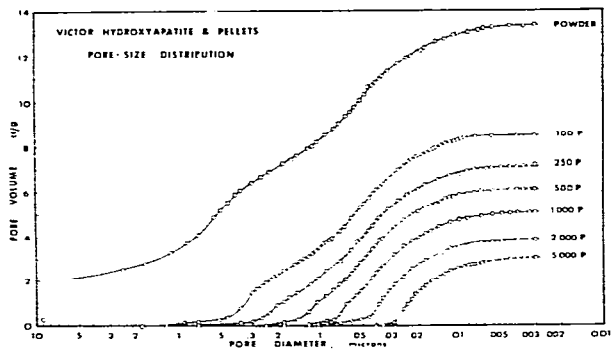

Fig. 5. Family of pore size distribution curves for Victor hydroxyapatite powder and compacts formed at loads up to 5000 psi (5000P) on a ½-in. die as indicated on the curves.

3.11 g/cm^3 for TVA-HAP. The individually measured real densities may not be as reliable in determining the true density of the solid in compaction as the above method, unless it was known that all of the open and closed void volume had been included. As shown in Fig. 2, the real density of VIC-HAP compacts was not constant over the load range investigated, but diminished rapidly with the applied force, reflecting the closing of some pore volume which became inaccessible to the intrusion of mercury. The measured real density is therefore not the same as the true density of the solid. The densities differ by a fraction due to the closed pore volume. It is suggested that the above is a good alternative method for establishing the value of the true density of the powdered solid used in the compaction study.

3.3 Pore size distributions of hydroxyapatite powders and compacts

3.3.1 VIC-HAP

Further characterization of hydroxyapatite powders and porous compacts formed under various pressures was obtained by mercury porosimetry [7-10]. The family of pore size distribution curves of VIC-HAP powder and compacts formed at applied loads of 100 - 5000 lb. (corresponding to pressures of 500 psi to 25,000 psi) are plotted in Fig. 5.

The bimodal pore size distribution of the pore volume is evident for the VIC powder. The disappearance of the first mode on compaction with increasing loads can be clearly seen. The first mode appears to vanish at compaction loads of 2000 lb. These curves also display the symmetry and uniformity of the reduction in total pore volume with increase in pressure and the decrease in size of the pores. The width of the distribution also diminishes evenly. The higher end of the pore size distributions is regularly diminished with increasing load.

The mercury porosimeter is a useful tool for characterizing powders and solids to derive graphic displays of their void or pore volume space and the distribution of the pore size, since the volume of mercury intruded into the sample under pressure is a direct measure of the void or the pore space within the sample. It is important to differentiate between the two terms, voids and pores. The empty spaces between particles, as in powders, are called voids. A single rigid solid, like a rock, a granule, or a compact, by definition has no voids. The open spaces within the solid specimen are called pores. Pores can be holes, fissures, cracks, or crevices within the structure of the solid specimen, whether it consists of a single piece or many chunks and bits. Consequently, powders can also be made up of particles which themselves have open spaces or pores, in which case both the void and the pore space must be taken in account.

Summary data for VIC-HAP powder and compacts obtained by mercury porosimetry are listed in Table 3. Pore volume, percent porosity, bulk density, density (real), and surface area are tabulated. Also included are the pore diameters, mean (50%) and the average ($4V/A$), for both pressurization and the depressurization data (Fig. 6).

The median pore diameters were obtained at the 50% value of the pore size distribution curves. The average ($4V/A$) pore diameter was calculated, assuming that all the pores were cylindrical in shape. Under this geometrical condition, the average pore diameter (D) in μm equals four times the total pore volume (V) in cm^3/g divided by the specific area (A) in m^2/g of the pores. The total pore volume was obtained from the porosimeter data; the surface area can be obtained from either the porosimeter data [10], as was done here, or from the independent determination of the nitrogen (B.E.T.) adsorption isotherm [11]. The computer program [12] for reduction of the raw data from the mercury porosimeter

TABLE 3
Mercury porosimetry data on compacts of Victor hydroxyapatite

No.	Sample	Pore volume (cm^3/g)	Porosity (%)	Bulk density (g/cm^3)	Density (g/cm^3)	Surface area* (m^2/g)	Pore diameter Pressure Median (μm)	Pore diameter Pressure Average (μm)	Pore diameter Depressure Median (μm)	Pore diameter Depressure Average (μm)
1	VIC-HAP	1.505	73.2	0.486	1.82	77.5	0.351	0.0624	23.6	0.132
2	VIC-HAP	1.337	78.3	0.586	2.70	72.4	0.266	0.0594	1.82	0.194
3	VIC-100P	0.849	71.9	0.825	2.758	71.9	0.0743	0.0456	0.205	0.140
4	VIC-250P	0.719	66.5	0.925	2.757	72.3	0.0571	0.0338	0.172	0.102
5	VIC-500P	0.612	62.6	1.023	2.736	72.5	0.0486	0.0322	0.147	0.0982
6	VIC-1000P	0.508	57.7	1.139	2.721	73.0	0.0377	0.0252	0.101	0.0754
7	VIC-2000P	0.388	50.3	1.295	2.700	69.4	0.0283	0.0204	0.0751	0.0652
8	VIC-3000P	0.358	48.9	1.365	2.669	69.2	0.0261	0.0206	0.0699	0.0598
9	VIC-5000P	0.306	45.8	1.497	2.760	69.6	0.0200	0.0146	0.0516	0.0430

* B.E.T. nitrogen surface area of VIC-HAP is 70.4 m^2/g.

with sample data calculations has been published.

It should be noted that the pressurization data from mercury intrusion yields information about the size of the opening of the voids or pores, and does not reflect the shape or pore size behind the "neck". Because of hysteresis, an estimate can be obtained from depressurization data of the average spherical diameteresis, an estimate can be obtained from depressurization data of the average spherical diameter of the space behind the neck through

The difference between the values of the median and the average pore diameters should also give an indication of the quality of the approximation attained by the assumption of cylindrical geometry of the pores in calculating the average pore diameter. The median and the average pore diameter data in Fig. 6 appear to be converging more for the depressurization than for the pressurization data. This observation indicates that the main body of the compact pores may attain more regular "spherical" shapes with increasing compaction than do the "necks". Any change in the relative shape of the "neck" openings of the pore space would not be indicated by these curves.

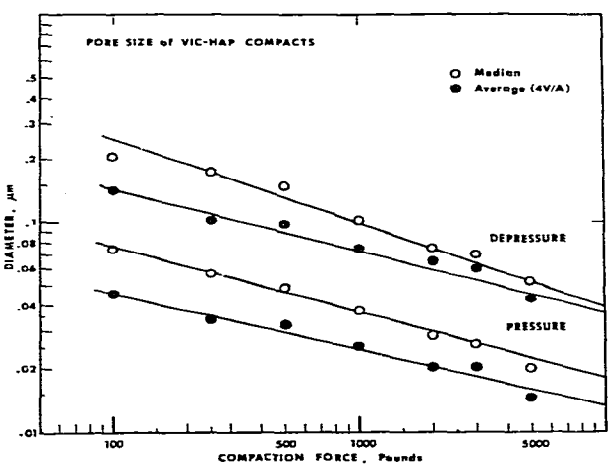

Fig. 6. Median and average ($4V/A$) pore diameters of VIC-HAP compacts for pressure and depressurization data *vs.* compaction force.

The first two samples in Table 3 are those of VIC-HAP powder. Both samples were treated similarly prior to running the mercury porosimeter; however, they yielded somewhat different pore volumes, bulk densities, and pore diameters. This observation further confirms the opinion that the packing conditions for a powder sample are difficult to control. From Table 3 it is also seen that there was no significant change in the surface area of compacts up to 1000P, after which it dropped significantly. Although no structural strength data were obtained on these compacts, it can be stated that a compact formed at a 1000-lb. load is quite strong, can withstand handling, and is not friable. The average Knoop hardness of a VIC-HAP pellet, made at 10,000-lb. load, and measured with a 200-g load on the diamond indenter was 28.5 kg/mm^2 for six measurements on two different compacts.

3.3.2 TVA-HAP

Mercury porosimeter data for TVA hy-

TABLE 4
Mercury porosimeter data on compacts of TVA hydroxyapatite

No.	Sample	Pore volume (cm^3/g)	Porosity (%)	Bulk density (g/cm^3)	Density (g/cm^3)	Surface area* (m^2/g)	Pore diameter Pressure Median (μm)	Pore diameter Pressure Average (μm)	Pore diameter Depressure Median (μm)	Pore diameter Depressure Average (μm)
1	TVA-HAP	0.975	74.5	0.765	3.00	3.13	9.24	1.24	21.7	3.29
2	TVA-HAP	0.874	73.0	0.835	3.09	2.52	6.84	1.39	16.7	9.08
3	TVA-HAP	0.776	70.7	0.911	3.11	3.17	5.11	0.77	9.51	1.71
4	TVA-500P	0.423	55.5	1.312	2.95	1.63	1.90	1.04	4.21	1.68
5	TVA-1000P	0.358	52.2	1.459	3.05	2.90	1.32	0.495	5.03	1.57
6	TVA-2000P	0.300	47.8	1.593	3.05	2.83	1.01	0.424	3.68	1.52
7	TVA-3000P	0.259	44.2	1.705	3.06	3.02	0.812	0.344	1.87	0.782
8	TVA-5000P	0.223	40.6	1.816	3.05	3.14	0.625	0.284	2.63	0.721

* B.E.T. nitrogen surface area of TVA-HAP powder is 3.02 m^2/g.

droxyapatite powder and compacts are summarized in Table 4. The first three samples listed in the table are powders. Again the variations in pore volume and porosity, bulk density, and especially pore diameters are evident. Since TVA powder was much coarser than VIC and apparently somewhat harder, compacts formed at loads less than 500P did not have adequate strength to withstand handling. The TVA-1000P compact, although not as strong as the VIC-1000P compact, had adequate strength to withstand handling; it had a porosity of 52.2%, which was close to the porosity (57.7%) of VIC-1000P.

As expected, pore volumes and porosities decreased and the bulk densities increased with pressure during compaction. Density of the solid remained constant within experimental error over the pressure range. The surface areas of the compacts appeared to show some reduction from powder to the 2000P compact, and then returned to normal again for the 3000P and the 5000P compacts. This effect may be a result of closed pores created at medium pressures, as was the case with VIC-HAP (Fig. 3) which later filled and disappeared at higher pressures (5000P).

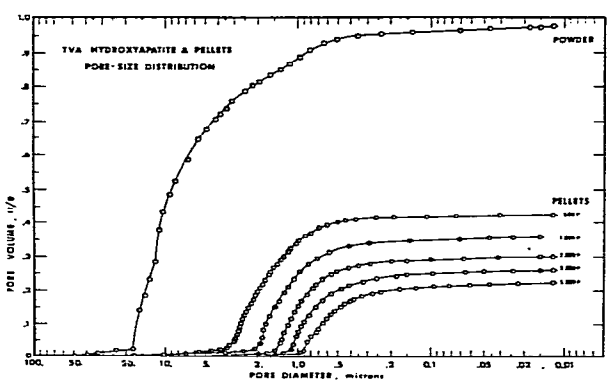

Fig. 7. Family of pore size distribution curves for TVA-HAP powder and compacts formed at loads up to 5000 lb. (5000P) on a ½-in. die as indicated on the curves.

The family of cumulative pore size distribution curves of TVA-HAP powder and compacts are plotted in Fig. 7. In contrast to VIC-HAP (Fig. 5), the TVA-HAP curves are shifted by a decade to larger pore sizes on the abscissa. This shift is the result of the larger particle size of TVA-HAP. The difference in the shape of the curves and the pore size distribution for the TVA- and VIC-HAP powders should be noted.

The pore diameters in Table 4 are plotted for TVA-HAP in Fig. 8. Median and average ($4V/A$) pore diameters of the compacts are plotted as a function of compaction force for both pressurization and depressurization conditions. The scatter of the depressurization values is a little greater than that of the pressurization values, but both sets of data appear to decrease uniformly in a parallel or slightly converging relationship. Since these data were from single experiments only, the scatter was not excessive. For example, the average pore diameter for the 500P compact from pressurization data was 1.04 μm, which is out of line with other data in Fig. 8. This variation is a result of using the experimental surface area value of 1.63 m^2/g, instead of an expected value of about 3 m^2/g in the calculation. If,

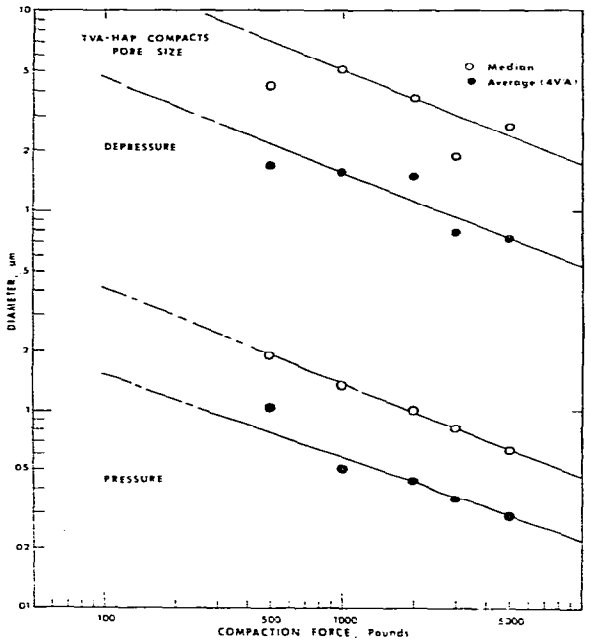

Fig. 8. Median and average ($4V/A$) pore diameters of TVA-HAP compacts *vs.* log of compaction force from pressurization and depressurization data.

for example, the surface area had been 2.9 m^2/g, the value obtained for 1000P compact, an average pore diameter of 0.6 μm would have been obtained. This value for the average pore diameter would have fallen on the pressurization line.

3.4 Pore size distribution of VIC-500P compacts sintered from 200° to 1000°C

The effect of drying and heat-treatment on hydroxyapatite compacts was investigated using VIC-HAP compacts formed at 500 lb. (500P). All compacts had the same "green" bulk density of about 1.00 g/cm^3 determined from pellet geometry. Compacted samples were placed in porcelain boats and isothermally sintered in a tube furnace for periods of 12 to 24 hours in a slow stream of nitrogen. After sintering, they were cooled in a desiccator and the densities and pore size distributions determined by mercury porosimetry.

Porosimeter data for VIC-500P compacts sintered at nine different temperatures are summarized in Table 5. The pore volume, percent porosity, bulk density and density remained unchanged up to 600°C. The surface area and the median and average pore diameters for both the pressurization and depressurization data, however, changed significantly at 500°C. The temperature could thus be raised to 600°C without any noticeable volume change or sintering effect, but the temperature could not be raised above 400°C without affecting the surface area or the median and the average pore diameters.

The above data can be examined in a different way in order to observe the physical changes in these compacts during sintering. The densification parameter (ΔD) is one way of investigating small changes, where the differential density ratio between the "green" and the sintered densities is compared with the difference between the true solid density and the "green" density:

$$\Delta D = \frac{D_s - D_0}{D_m - D_0}$$

where D_s = sintered density, D_0 = "green" density (2.736 g/cm^3), and D_m = "true solid

TABLE 5
Mercury porosimetry data on VIC-500P hydroxyapatite compacts sintered from 200° to 1000°C in nitrogen

No.	Sintering temp. (°C)	Pore volume (cm^3/g)	Porosity (%)	Bulk density (g/cm^3)	Density (g/cm^3)	Surface area (m^2/g)	Pore diameter Pressure Median (μm)	Pore diameter Pressure Average (μm)	Pore diameter Depressure Median (μm)	Pore diameter Depressure Average (μm)
1	200	0.639	63.7	0.996	2.74	70.9	0.0514	0.0318	0.155	0.0983
2	300	0.636	64.0	1.005	2.79	72.4	0.0507	0.0323	0.173	0.110
3	400	0.638	63.8	1.000	2.76	71.3	0.0518	0.0332	0.166	0.112
4	500	0.626	62.6	1.000	2.67	65.5	0.0550	0.0375	0.224	0.152
5	600	0.636	63.5	0.999	2.74	53.1	0.0642	0.0479	0.241	0.193
6	700	0.603	61.7	1.026	2.68	38.5	0.0762	0.0625	0.327	0.308
7	800	0.587	63.0	1.073	2.90	28.1	0.0931	0.0834	0.467	0.463
8	900	0.536	61.9	1.157	3.05	14.3	0.163	0.146	0.918	0.949
9	1000	0.512	60.7	1.185	3.02	7.11	0.298	0.272	3.323	2.321

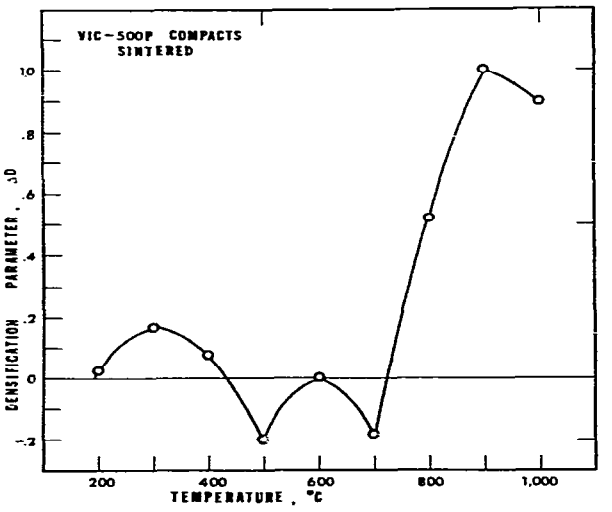

Fig. 9. Densification parameters for VIC-500P compacts sintered at temperatures from 200° to 1000°C.

density" (3.05 g/cm^3). The densification parameter (ΔD) is plotted in Fig. 9 as a function of sintering temperature. If no change resulted during sintering, the data should fall near the zero line, as occurred at 200° and 600°C.

Pore size distribution curves were measured for the sintered compacts and are plotted in Figs. 10 and 11. For better internal comparison between the pore size distribution curves of the compacts, and for the visual indication of the pore size distribution changes, the data were plotted in percent on the ordinate. There appeared to be little change in the percent pore volume distribution curves (Fig. 10) for the curves at 200°, 300° and 400°C

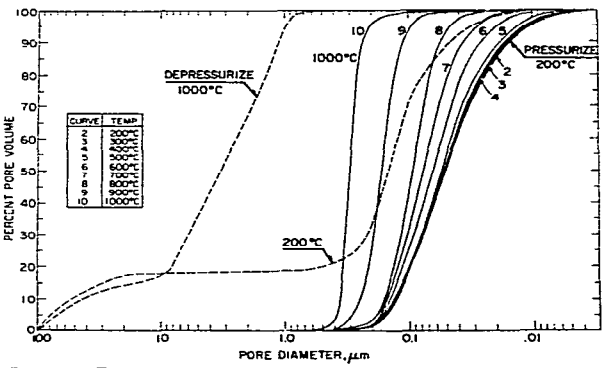

Fig. 10. Percent pore volume *vs.* pore diameter curves, *i.e.* cumulative pore size distribution curves for VIC-500P compacts sintered at 200° - 1000°C in nitrogen atmosphere. The range of hysteresis from the depressurization data is shown by the two broken line curves.

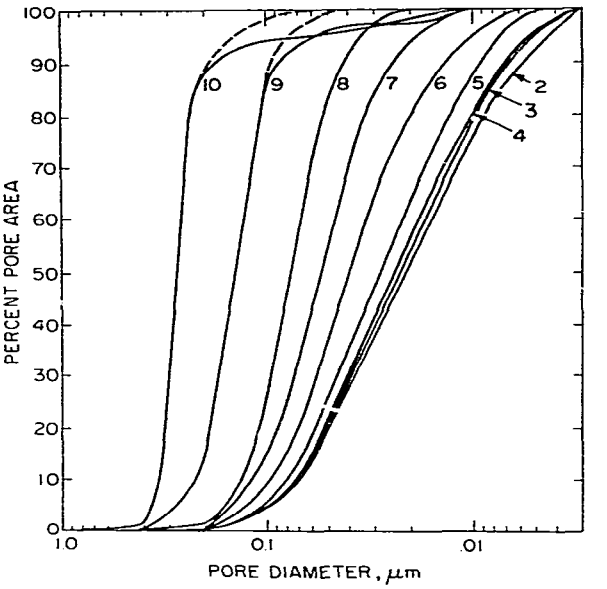

Fig. 11. Cumulative percent pore area *vs.* pore diameter distribution curves for VIC-500P compacts sintered at temperatures of 200° (curve 2) to 1000°C (curve 10) in 100° increments in nitrogen.

(marked 2, 3, 4). If the curves are examined carefully, subtle differences are evident at small pore diameters between 0.005 and 0.05 μm. The differences, however, were not great enough to affect the percent porosity or the density data.

When the cumulative percent pore area curves (Fig. 11) were compared, the small differences, observed in the low temperature curves, were magnified. This magnification is caused mainly by the fact that small pores have a greater affect on area and its distribution than on pore volume and its distribution.

The ranges of the hysteresis for the sintered compacts are shown in Fig. 10 and are defined by the broken line curves for the depressurization data of 200°- and 1000°C-sintered compacts.

With increased sintering temperatures, the pore size distribution curves from the pressure data became more vertical at each increment. The distribution of pore openings became more uniform, narrower in distribution, and larger in size, as the temperature increased. The median pore size for the pressurization data increased about six-fold, from 0.05 μm at 200°C to 0.30 μm at 1000°C, whereas about a twenty-fold increase in the median pore diameter for the depressurization data

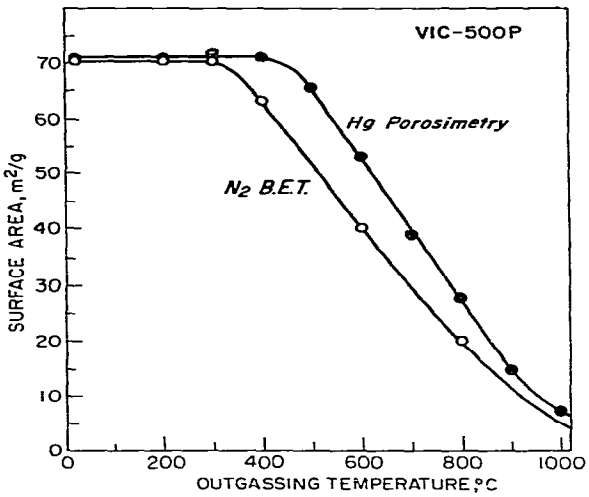

Fig. 12. Surface areas of VIC-500P compacts *vs.* outgassing temperature. Areas measured by nitrogen adsorption are labeled N_2 B.E.T., and other areas were calculated from mercury porosimeter data.

occurred, from 0.15 μm at 200°C to 3.3 μm at 1000°C. Although there was a shift in pore size, the distribution of pores appeared to remain relatively unchanged.

The surface areas of VIC-500P compacts from mercury porosimetry and nitrogen adsorption are shown in Fig. 12. A sudden drop in surface areas was observed after 300°C or 400°C, depending on whether the B.E.T. nitrogen or the mercury porosimeter data was used.

The temperature coefficient (dA/dT) for the sintering of the specific surface of VIC-HAP was measured from the slope of the nitrogen B.E.T. surface area curve, and was found to be about 0.11 $m^2\ g^{-1}\ deg^{-1}$ for the temperature range between 500° and 900°C. Correspondingly, the surface area change with the change in outgassing temperature (dA/dT) was about 0.13 $m^2\ g^{-1}\ deg^{-1}$ for the compacts measured by mercury porosimeter between 400° and 800°C. Although the initial temperatures for each set of data were different, the coefficients were about the same.

Another means of examining the change in pore area on sintering is to compare the changes in pore area with pore volume (Fig. 13). The samples heated at low temperatures are at the upper right-hand side of the figure. With increasing temperature, as pore

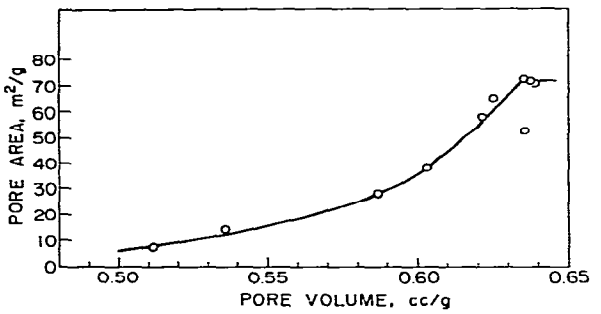

Fig. 13. Pore area *vs.* pore volume for sintered VIC-500P compacts.

area and volume decreased, the values decreased toward the origin of the curve. The slopes indicate that there may be at least two different rates operating during the sintering process. It was observed that changes in pore area compared with volume (dA/dV) were much more rapid (1028 m^2/cm^3) at low temperatures than at high temperatures (280 m^2/cm^3), by a factor of 3.7.

Another means of examining the physical changes of the sintered compacts is to determine whether a relationship exists between the change in pore volume and the bulk density. It was also of interest to establish whether a change of pore volume of the compact affected only the internal arrangement and size distribution of the pores, or whether it also involved the external change of the physical dimensions of the compact. Figure 14 shows that after sintering at 600°C the decrease in the pore volume was accompanied by a corresponding increase in bulk density. The increase clearly illustrates that the exter-

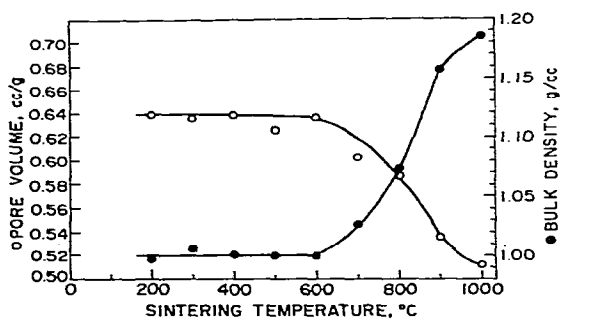

Fig. 14. Pore volume and bulk density curves for VIC-500P sintered compacts as a function of sintering temperature.

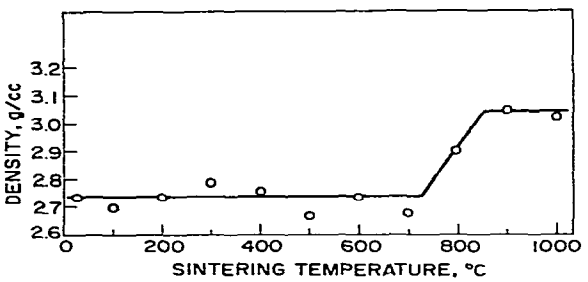

Fig. 15. Density of the VIC-500P compacts sintered from 200° to 1000° C as a function of sintering temperature.

nal shrinkage in size of the compact is accompanied by a corresponding decrease of internal open pore volume.

Changes in physical parameters of the sintered compacts were temperature dependent. Surface areas decreased after 300° C or 400° C. Pore volume and the bulk density did not change noticeably until after 600° C. Real density of the solid, by mercury porosimetry, remained constant up to 700° C (Fig. 15), above which significant changes appeared. Pore area proved to be the most sensitive indicator of change for following the effect of outgassing temperature on the sample compacts, and for determining the temperature limit for outgassing the sample without any sintering effects.

A plot of pore diameter data of sintered VIC-500P is shown in Fig. 16, where the median and the average pore diameters for both pressurization and depressurization data show convergence with increasing sintering temperature. As the sintering of compacts progressed, the average pore diameter approached the median pore diameter. Thus the average pore diameter became a fair estimate of the median pore diameter of the sintered compact. An attempt to emphasize this observation is made in Fig. 16, where the ratio of the median to average (Med/Av) pore diameter is plotted for the depressurization data. The change in the ratio took place between 500° and 700° C, where the ratio became one. A change took place in the same temperature range for the pressurization data.

These results indicate that pores, both openings ("necks") and the main body, are smoothed-out and rounded-off. In the course of sintering, the surface tension of the solid, and the surface flow of the hydroxyapatite

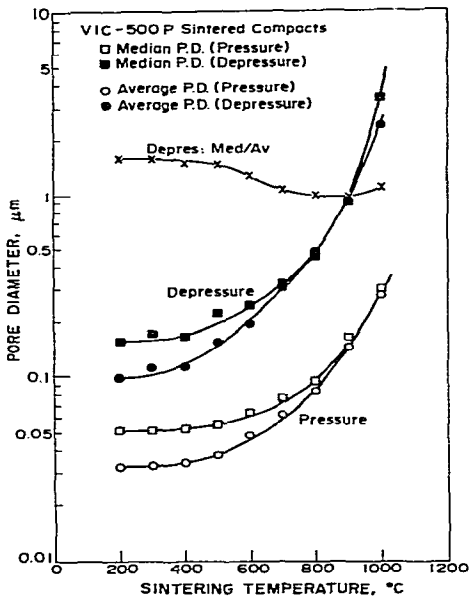

Fig. 16. Median and average ($4V/A$) pore diameters for VIC-500P compacts sintered from 200° to 1000° C *vs.* sintering temperature. Also, at the top of the figure, the ratio (Med/Av) is plotted for the depressurization data.

are "smoothing" out the rough irregular pores originally created during compaction. These factors contribute to a more uniform size, rounded shape, and homogeneous distribution of pores.

CONCLUSIONS

The following significant information about compactibility of two different hydroxyapatite powders (VIC- and TVA-HAP) has been obtained.

(1) Bulk density measurements made by using a micrometer to measure thickness of the compacts were 1 - 2% higher than the bulk densities derived from mercury porosimeter data. This agreement was a good check on both measurements for bulk density, and it established a basis for reliability for further calculations of the porosimeter data.

(2) It was possible to form compacts with varying porosities from HAP powders. Linear relations between log of applied load and pore volume and between the pore volume and bulk density were established. Pore volume and size distribution at a given load depend

largely on the particle size distribution of the powder. The pore size distribution and median pore diameter decreased linearly with the logarithm of the applied load.

(3) Interpretation of the pore size distribution curves is greatly enhanced by measuring the extent of hysteresis of the depressurization curves. Pressurization curves gave size distributions of pores according to openings ("necks") of the accessible open volumes regardless of the shape or size of the pore or void behind it. Depressurization curves from the porosimeter conversely yielded size distributions of the effective mean size of open spaces behind the "necks". To avoid misinterpretation of the mercury porosimeter data, both pressurization and depressurization curves should be run.

(4) Surface areas of hydroxyapatite compacts are reduced by sintering above 300° - 400°C. This effect was also reflected in the area distribution changes of compacts sintered above 400°C. Sintering of VIC-500P compacts above 400°C resulted in narrowed pore size distributions and increased diameters of the pore. Densification of compacts occurred above 700°C.

ACKNOWLEDGEMENTS

This study was supported by Training Grant DE-00181 from the National Institute for Dental Research, National Institutes of Health, Bethesda, Md.

REFERENCES

1 H. Sicher (ed.), Orban's Oral Histology and Embryology, Mosby, St. Louis, 5th edn., 1962, p. 53.
2 M.I. Kay and R.A. Young, Crystal structure of hydroxyapatite, Nature, 204 (1964) 1050—1052.
3 R.A. Young and J.C. Elliott, Atomic-scale bases for several properties of apatites, Arch. Oral Biol., 11 (1966) 699—707.
4 S.F. Hulbert, F.A. Young, R.S. Mathews, J.J. Klawitter, C.D. Talbert and F.H. Stelling, Potential of ceramic materials as permanently implantable skeletal prostheses, J. Biomed. Mater. Res., 4 (1970) 433—456.
5 R.G. Topazian, W.B. Hammer, C.D. Talbert and S.F. Hulbert, The use of ceramics in augmentation and replacement of portions of the mandible, J. Biomed. Mater. Res., 6 (1972) 311—332.
6 W.J. Clarke, T.D. Driskell, C.R. Hassler, V.J. Tennery and L.R. McCoy, Calcium phosphate resorbable ceramics: A potential alternative to bone grafting, Abstr. Program and Abstracts of Papers, Int. Assoc. Dent. Res., 51st General Meeting, Washington, D.C., April 1973, paper 259, p. 123.
7 H.M. Rootare, A short literature review of mercury porosimetry as a method of measuring pore size distributions in porous materials, and a discussion of possible sources of errors in this method, Aminco Lab. News, 24 (Fall 1968) 4A—4H.
8 H.M. Rootare, A review of mercury porosimetry, in J.S. Hirschhorn and K.H. Roll (eds.), Advanced Experimental Techniques in Powder Metallurgy, Plenum Press, New York, 1970, pp. 225—252.
9 C. Orr, Jr., Application of mercury penetration to materials analysis, Powder Technol., 3 (1969/70) 117—123.
10 H.M. Rootare and C.F. Prenzlow, Surface areas from mercury porosimeter measurements, J. Phys. Chem., 71 (1967) 2733—2736.
11 Stephen Brunauer, P.H. Emmett and Edward Teller, Adsorption of gases in multimolecular layers, J. Am. Chem. Soc., 60 (1938) 309—319.
12 H.M. Rootare and Judson Specner, A computer program for pore volume and pore area distribution calculations from mercury porosimeter data on particulate or porous materials, Powder Technol., 6 (1972) 17—23.